PCCP

RSC Publishing

COMMUNICATION

How the number of fitting points for the slope of the mean-square displacement influences the experimentally determined particle size distribution from single-particle tracking

Dominique Ernst and Jürgen Köhler*

The size distribution of nanoparticles can be determined by single-particle tracking. This yields the mean-squared displacement (MSD) as a function of the lag time, and for normal diffusion the slope of this curve is directly related to the diffusion coefficient or *via* the Stokes–Einstein relation to the particle size. Here we demonstrate how the experimentally determined size distributions are affected by the number of fitting points used to determine the slope of the MSD curve.

In recent years, nanoparticles from various materials have become an interesting object of research, because they offer extraordinary properties that might be relevant for electronics, functional surfaces, or pharmaceutical applications, to name a few. Many of these applications require a reliable and fast method to determine the size distribution of the particles. Next to practical issues this is important to judge the hazardous potential of the nano-sized objects, which is determined by a combination of physico-chemical properties, and among which the particle size plays an important role. Unfortunately, the most accurate methods to determine this parameter, such as electron microscopy, are expensive and time consuming due to lengthy sample preparations, whereas other methods that are fast and cheap, such as dynamic light scattering, lack the requested precision when the size distribution of the particles is multi modal.[1] Alternative approaches exploit the dependence of the diffusion (Brownian motion) on the particle size, and have been applied successfully in the life sciences. Here, the ensemble-based methods take advantage of the fact that the bioparticles feature a uniform size distribution, as for example studying a distinct protein.[2,3] For multi-modal size distributions of the particles these methods fail as well, and had to be extended to follow the diffusion of the particles on an individual basis.[4–7] As a consequence of this, following the diffusion of single nanoparticles and analysing the characteristics of their

Brownian motion has become an important tool to determine the size distribution of nano objects, which is commonly referred to as single-particle tracking (SPT).

All the different techniques that have been developed for SPT[4,8–14] have in common, that they record the position of a particle as a function of time which provides the trajectory $r(t)$. Most commonly these trajectories are analysed in terms of the mean-squared displacement (MSD) as a function of the lag time τ. For a 2-dimensional normal diffusion process the MSD generally scales linearly in time, according to $\mathrm{MSD}(\tau) = 4D\tau$, where D is the diffusion coefficient that is related to the particle size *via* the Stokes–Einstein relation, $D = \dfrac{k_{\mathrm{B}}T}{6\pi\eta a}$. Here $k_{\mathrm{B}}T$ refers to the thermal energy, η to the viscosity and a to the radius of the particle. Hence, from a simple linear fit of the MSD curve the diffusion coefficient and concomitantly the radius of the diffusing particle can be obtained.

The mathematical background for this analysis is known already for a very long time.[15–17] Yet, in an experimental situation the actually measured MSD curve is influenced by experimental shortcomings such as the limited localisation accuracy of the data points of the trajectory, noise, or the finite length of the trajectory. As a consequence of this, the accuracies of the data points of the MSD curve vary with respect to each other. It has been shown that the optimum accuracy for the diffusion coefficient can be achieved by taking only the first few data points of an MSD curve into consideration to fit its slope.[16,18] This reflects the fact that for increasing lag times the accuracy of the data points in the MSD decreases due to the progressively decreasing averaging of the available data. Taking too many data points into account for fitting the slope of the MSD curve therefore leads to a deterioration rather than an improvement of the result. Yet, the very first data points of the MSD are affected by blurring of the position of the particle during data acquisition, and other localisation errors. These shortcomings average out for MSD points that correspond to longer lag times.[19] Here we compare the outcome for the particle size distributions that are obtained from the same data

Experimental Physics IV and Bayreuth Institute for Macromolecular Research (BIMF), University of Bayreuth, 95440 Bayreuth, Germany.
E-mail: juergen.koehler@uni-bayreuth.de

This journal is © the Owner Societies 2013

Phys. Chem. Chem. Phys., 2013, **15**, 3429–3432 | **3429**

set for evaluating the MSD curves with an optimised number of fitting points and for an arbitrarily chosen number of fitting points. It is found that the proper choice of the number of fitting points for the slope of the MSD curve has a crucial impact on the measured particle size distributions.

As nanoparticles we used beads with a diameter of 20 nm that were loaded with nile red as fluorophore (molecular probes, 20 mg ml^{-1} dissolved in water). The commercial solution was diluted in water and mixed with glycerol (Sigma) until a concentration of 2 pM was achieved for the tracer particles. A small drop of this solution was sandwiched between two clean coverslips and sealed with vacuum grease (High-Vacuum Grease, Wacker) to avoid a flow field. This sample was mounted on a 3-axis piezo stage (Tritor 102, piezosystem Jena), and illuminated with the output from an Ar/Kr-ion laser (Innova 70C Spectrum, Coherent) that was operated at 514 nm. In order to follow the diffusion of the particles we employ orbit tracking[20] which is accomplished by guiding the light through a deflection unit consisting of two mutually perpendicularly arranged acousto optical deflectors (AOD, DTSX-400-532, Pegasus). The light orbit is projected towards an infinity-corrected water-immersion objective (UPLSAPO, 60×, NA = 1.2, Olympus) *via* a dichroic beam splitter (z532RDC, AHF). The waist of the focussed laser beam was 270 nm. The radius and the rotation frequency of the orbit were adjusted to 190 nm and 1 kHz, respectively.

The emission from a fluorescent nanoparticle was collected with the same objective, passed the dichroic and a dielectric optical filter (HQ545LP, OD = 6 @ 514 nm, AHF), and was focussed on an avalanche photo diode (SPCM-AQR-14, Perkin Elmer).

From the modulation of the emission intensity of the particle due to the rotating laser focus a feedback signal is generated that provides the position of the bead with high accuracy in the lateral dimensions. The temporal resolution of the experiments is Δt = 4 ms. More details about the setup and the data evaluation can be found elsewhere.[20] In particular, all MSD points have been fitted with a linear function including an offset that stems from the finite position accuracy (although this offset was irrelevant for the slope of the MSD curve and the resulting diffusion coefficient/particle radius). All experiments are performed at room temperature, *i.e.* 21 ± 0.5 °C.

We recorded trajectories consisting of about 1.5×10^5 positions from seven different individual polymer beads. From the recorded trajectories we calculated the time-averaged MSDs, the first 50 data points of which are shown in Fig. 1. The MSD curves show a linear variation as a function of the lag time and feature different slopes. For our setup the optimum result for fitting the slope of the MSD curves is obtained by taking into account only the data points 2–5. Interestingly, this choice represented a most optimal solution that did not depend on the length of the trajectories as detailed in ref. 19. The resulting time-averaged diffusion coefficients, $\langle D \rangle_{\mathrm{T}}$, extracted from these data are summarized in Table 1.

The diffusion coefficients $\langle D \rangle_{\mathrm{T}}$ show strong variations and cover the range from about 12×10^{-3} µm^2 s^{-1} to 26×10^{-3} µm^2 s^{-1}. Since all 7 MSDs represent highly averaged data, it is very unlikely
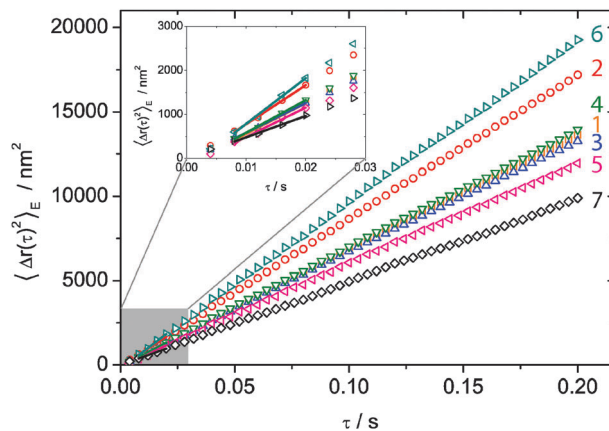

Fig. 1 Time-averaged MSDs (first 50 data points) of the 7 individual trajectories from 20 nm sized beads diffusing in pure glycerol. For each bead, trajectories were recorded for 10 minutes with a time increment of Δt = 4 ms. The inset displays the first 7 data points of each MSD and the linear fits (full lines) to the data points 2–5, *i.e.* for using n = 4 fitting points.

Table 1 Summary of the results from the MSDs from 7 individual polymer beads. The entries denote the diffusion coefficient, $\langle D \rangle_{\mathrm{T}}$, from the time-averaged MSDs from the long trajectories, and corresponding bead radius $\langle a \rangle_{\mathrm{T}}$ as obtained from the Stokes–Einstein relation. The indices indicate the time-averaging

Trajectory number	$\langle D \rangle_{\mathrm{T}}/10^{-3}$ µm^2 s^{-1}	$\langle a \rangle_{\mathrm{T}}$/nm
1	17.45	10.3
2	22.20	8.1
3	16.86	10.6
4	18.54	9.7
5	16.76	10.7
6	26.02	6.9
7	12.19	14.7

that these variations result from a lack of statistics, and it is reasonable to assume that this reflects the differences in the size of the individual beads that have been traced. Hence, interpreting the experimentally determined diffusion coefficients $\langle D \rangle_{\mathrm{T}}$ as "correct", they can be used as input for the Stokes–Einstein relation to determine the actual size of the polymer beads. The results for the particle radii $\langle a \rangle_{\mathrm{T}}$ are listed also in Table 1, featuring an arithmetic mean of 10.14 nm and a standard deviation of 2.47 nm, which is in reasonable agreement with the information provided from the manufacturer (a = 10 ± 2 nm).

In the following we will illustrate how the number of fitting points that are taken into account to determine the slope of the MSD curve influences the experimental outcome. In order to obtain a statistically relevant ensemble of trajectories from the same particle, we cut each of the 7 long trajectories into a set of segments with 2000 data points per segment, which yields an ensemble of 75 trajectories per particle. Subsequently, we determined from each subtrajectory the time-averaged diffusion coefficient and the corresponding particle radius *via* the Stokes–Einstein relation. This protocol was carried out twice: once for the optimum choice of the number of fitting points, n = 4, and once for an arbitrarily chosen value of n = 50. Though, it is worth noting that even for n = 50 each of the MSD data points represents an average over 1850 entries. The resulting distributions for the
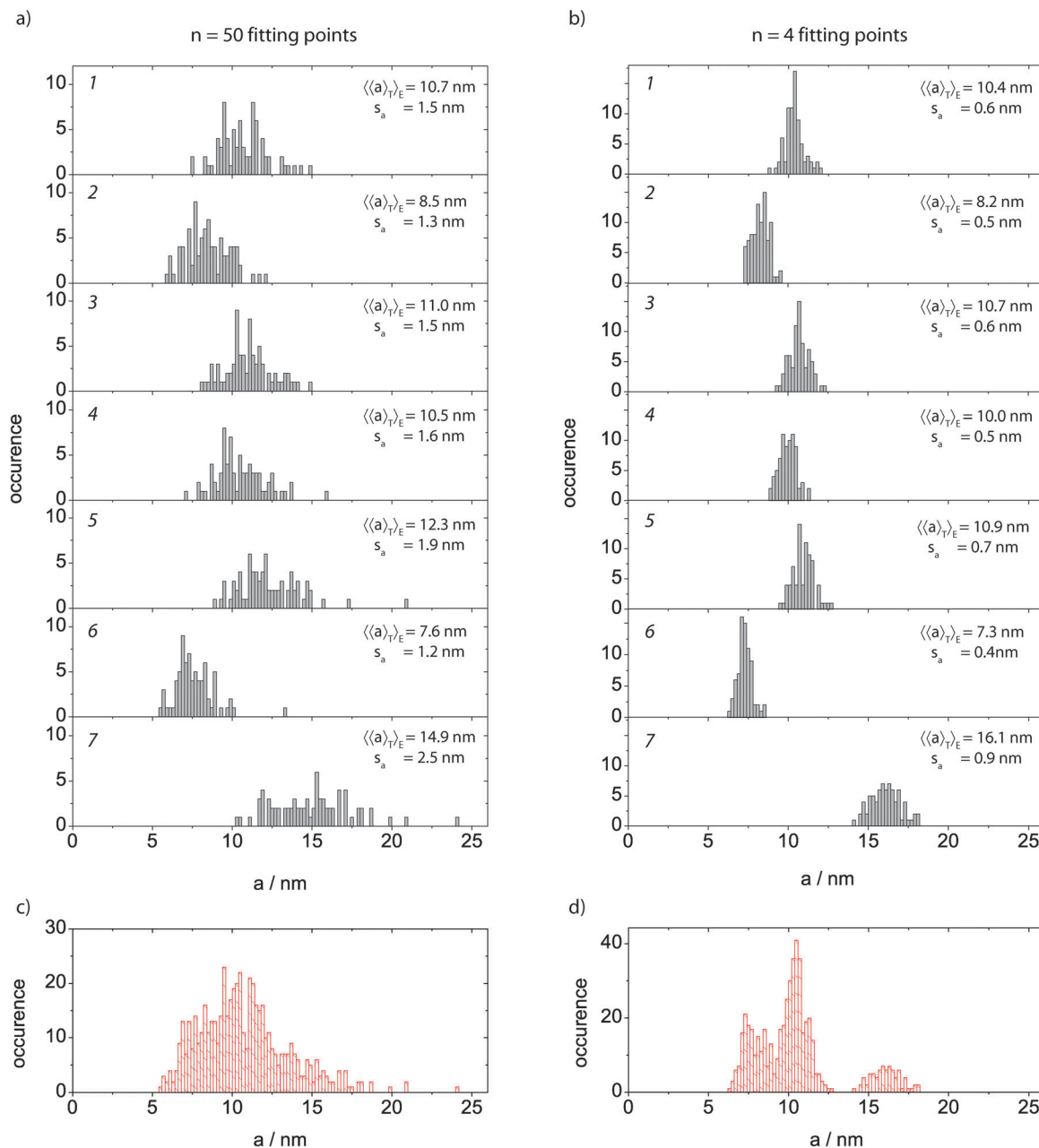
Fig. 2 Statistics of the determined particle sizes for the 7 different beads from 75 trajectories of 2000 particle positions each. The means $\langle\langle a\rangle_T\rangle_E$ and the (empirical) standard deviations s_a of these distributions are given in the figure. (a) Using the first 50 data points of the MSD curve to fit the slope, and (b) using data points 2–5 instead. (c) Merged histograms from (a). (d) Merged histograms from (b).

particle radii are compared in Fig. 2 for the two choices of the number of fitting points. Visual inspection already reveals that the histograms obtained for $n = 4$ are significantly narrower than those for the other case. This is confirmed by comparing the mean values, $\langle\langle a\rangle_T\rangle_E$, and the standard deviations s_a, as given in the figure and in Table 2.

At the bottom of Fig. 2 the individual histograms have been merged into a single histogram for each particular choice of the number of fitting points. For $n = 4$ three peaks can be clearly distinguished, whereas for $n = 50$ this substructure remains obscured. We want to emphasize again that both histograms

have been determined from the same data set, and differ only with respect to the evaluation of the MSD curves.

The individual histograms can be interpreted as the empirical probability density functions for measuring a distinct particle radius in one of the experiments. For our experimental conditions, an optimum evaluation of the MSD curves allows us to achieve a relative accuracy for the particle size of about 6%, whereas this drops for the same data to about 15% if a suboptimal number of points is chosen to fit the slope of the MSD. Yet, it should be kept in mind that trajectories with 2000 data points are generally considered as a large data set. For shorter trajectories the relative

This journal is © the Owner Societies 2013

Phys. Chem. Chem. Phys., 2013, **15**, 3429–3432 | **3431**

Table 2 Summary of the mean values $\langle\langle a\rangle_T\rangle_E$ and empirical standard deviations s_a of the individual particle radii distributions shown in Fig. 2. The indices indicate the ensemble-averaging of the time-averaged entries

Trajectory number	$\langle\langle a\rangle_T\rangle_E$/nm	s_a/nm	$\langle\langle a\rangle_T\rangle_E$/nm	s_a/nm
	$n = 50$		$n = 4$	
1	10.7	1.5	10.4	0.6
2	8.5	1.3	8.2	0.5
3	11.0	1.5	10.7	0.6
4	10.5	1.6	10.0	0.5
5	12.3	1.9	10.9	0.7
6	7.6	1.2	7.3	0.4
7	14.9	2.5	16.1	0.9

accuracy for determining the diffusion coefficient or likewise the particle radius from an MSD curve will decrease even further.[19]

These findings touch upon an important issue because commercial applications have been developed that measure the size distributions of nanoparticles by particle tracking.[1] In those experiments typically a large number of short trajectories (each one in the order of some hundreds of data points[21]) are measured. Then from each trace a diffusion coefficient and the corresponding size of the particle are determined. As our data show, the outcome of a single experiment can already vary significantly, represented by the probability density functions as shown in Fig. 2. Unfortunately, information about these probability density functions is usually not accessible. Since each trajectory stems from a different particle, and since the particles can vary in size, ensemble averaging over many trajectories will not be helpful either. The importance, however, of having reliable information about size distributions of nanoparticles is an emerging field in the context of health protection, in particular if one considers that up to now a well characterised safety protocol regarding the toxicity for the use of nanoparticles is still not in sight.[22]

Acknowledgements

References

1 V. Filipe, A. Hawe and W. Jiskoot, *Pharm. Res.*, 2010, **27**, 796–810.

2 E. L. Elson, *Annu. Rev. Phys. Chem.*, 1985, **36**, 379–406.

3 E. L. Elson, *Biophys. J.*, 2011, **101**, 2855–2870.

4 B. J. Schnapp, J. Gelles and M. P. Sheetz, *Cell Motil. Cytoskeleton*, 1988, **10**, 47–53.

5 B. W. Hicks and K. J. Angelides, *J. Membr. Biol.*, 1995, **144**, 231–244.

6 J. Gelles, B. J. Schnapp and M. P. Sheetz, *Nature*, 1988, **331**, 450–453.

7 Th. Schmidt, G. J. Schuetz, W. Baumgartner, H. J. Gruber and H. Schindler, *Proc. Natl. Acad. Sci. U. S. A.*, 1996, **93**, 2926–2929.

8 Q. Wang and W. E. Moerner, *ACS Nano*, 2011, **5**, 5792–5799.

9 V. Levi, Q. Ruan, K. Kis-Petikova and E. Gratton, *Biochem. Soc. Trans.*, 2003, **31**, 997–1000.

10 A. J. Berglund and H. Mabuchi, *Appl. Phys. B*, 2004, **78**, 653–659.

11 M. A. Thompson, M. D. Lew, M. Badieirostami and W. E. Moerner, *Nano Lett.*, 2009, **10**, 211–218.

12 M. Speidel, A. Jonáš and E.-L. Florin, *Opt. Lett.*, 2003, **28**, 69–71.

13 J. G. Ritter, R. Veith, J.-P. Siebrasse and U. Kubitscheck, *Opt. Express*, 2008, **16**, 7142.

14 H. Cang, C. S. Xu, D. Montiel and H. Yang, *Opt. Lett.*, 2007, **32**, 2729–2731.

15 H. Qian, M. P. Sheetz and E. L. Elson, *Biophys. J.*, 1991, **60**, 910–921.

16 X. Michalet, *Phys. Rev. E*, 2010, **82**, 041914.

17 M. J. Saxton, *Biophys. J.*, 1997, **72**, 1744–1753.

18 X. Michalet and A. J. Berglund, *Phys. Rev. E*, 2012, **85**, 061916.

19 D. Ernst and J. Köhler, *Phys. Chem. Chem. Phys.*, 2013, **15**, 845–849.

20 D. Ernst, S. Hain and J. Köhler, *J. Opt. Soc. Am. A*, 2012, **29**, 1277–1287.

21 Ch. Finder, M. Wohlgemuth and Ch. Mayer, *Part. Part. Syst. Charact.*, 2004, **21**, 372–378.

22 R. Landsiedel, L. Ma-Hock, A. Kroll, D. Hahn, J. Schnekenburger, K. Wiench and W. Wohlleben, *Adv. Mater.*, 2010, **22**, 2601–2627.